PRELIMINARY EXPERIMENTS WITH A TRIPLE-LAYER PHOSWICH DETECTOR FOR RADIOXENON DETECTION

Abi T. Farsoni, David M. Hamby, Chee S. Lee, and Anthony J. Elliott

Oregon State University

Sponsored by National Nuclear Security Administration

Contract No. DE-FC52-06NA27322
Proposal No. BAA06-36

ABSTRACT

The International Monitoring System (IMS) employs some special radiation detectors to monitor atmospheric or underground nuclear weapons tests around the world. These detectors should be able to detect ultra low concentrations of xenon radioisotopes in the atmosphere where the background level is relatively high. Exploiting the fact that the most interesting xenon radioisotopes (^{133}Xe, ^{133m}Xe, ^{131m}Xe, and ^{135}Xe) emit a beta or conversion electron (CE) in coincidence with an X-ray or gamma-ray, these detectors have been designed and optimized to record coincidence events from the radioxenon isotopes. The IMS currently uses detection systems in which beta/CE and X-ray/gamma-ray are measured in separate detectors (as in the Automated Radioxenon Sampler/Analyzer [ARSA] system developed at Pacific Northwest National Laboratory [PNNL]). Although experimental results show that the ARSA system is able to detect very low concentrations of radioxenon, its complexity makes the beta and gamma-ray energy calibration very difficult.

Phoswich technology, accompanied by digital signal processing of photomultiplier tube (PMT) pulses, can simplify radioxenon detection. If well designed, like other current sensitive radioxenon detectors, a phoswich detector is also capable of detecting beta/gamma coincidence events using digital-pulse-shape analysis. We have designed a two-channel triple-layer phoswich detector for radioxenon detection. Each phoswich detector consists of three scintillation layers: a thin plastic (1.5mm) scintillator for detection of beta and CE, a CaF_2 layer (2mm) for X-ray detection and a NaI layer (25.4mm) for gamma-ray measurement. A two-channel FPGA-based Digital Pulse Processor, DPP2.0, (250 MHz, 12 bits) has been designed and constructed for capturing and transferring valid phoswich pulses to the PC. A graphical user interface (GUI) also has been developed to control the DPP2.0, digitally analyze phoswich pulses, and reconstruct the 2-D beta/gamma coincidence spectra.

In this paper, our digital pulse shape discrimination technique, the DPP2.0, and the GUI are introduced. At the end, our preliminary measurements with the prototypic phoswich detector are discussed.

Report Documentation Page

Form Approved
OMB No. 0704-0188

1. REPORT DATE	2. REPORT TYPE	3. DATES COVERED
SEP 2008		**00-00-2008 to 00-00-2008**

4. TITLE AND SUBTITLE	5a. CONTRACT NUMBER
Preliminary Experiments with a Triple-Layer Phoswich Detector for Radioxenon Detection	5b. GRANT NUMBER
	5c. PROGRAM ELEMENT NUMBER
6. AUTHOR(S)	5d. PROJECT NUMBER
	5e. TASK NUMBER
	5f. WORK UNIT NUMBER
7. PERFORMING ORGANIZATION NAME(S) AND ADDRESS(ES) **Oregon State University,Corvallis,OR,97331-4501**	8. PERFORMING ORGANIZATION REPORT NUMBER
9. SPONSORING/MONITORING AGENCY NAME(S) AND ADDRESS(ES)	10. SPONSOR/MONITOR'S ACRONYM(S)
	11. SPONSOR/MONITOR'S REPORT NUMBER(S)

12. DISTRIBUTION/AVAILABILITY STATEMENT
Approved for public release; distribution unlimited

13. SUPPLEMENTARY NOTES
Proceedings of the 30th Monitoring Research Review: Ground-Based Nuclear Explosion Monitoring Technologies, 23-25 Sep 2008, Portsmouth, VA sponsored by the National Nuclear Security Administration (NNSA) and the Air Force Research Laboratory (AFRL)

14. ABSTRACT
see report

15. SUBJECT TERMS

16. SECURITY CLASSIFICATION OF:			17. LIMITATION OF ABSTRACT	18. NUMBER OF PAGES	19a. NAME OF RESPONSIBLE PERSON
a. REPORT **unclassified**	b. ABSTRACT **unclassified**	c. THIS PAGE **unclassified**	**Same as Report (SAR)**	**10**	

OBJECTIVE

To monitor atmospheric or underground nuclear weapons tests, special radiation detectors have been designed and employed for measuring the concentration of xenon radioisotopes in the atmosphere. In a high-level background environment, these detectors are capable of detecting very low amounts of radioxenon by employing a beta-gamma coincidence detection technique. Using this technique, the detection system updates the beta and/or gamma spectra only when the beta and gamma channels are triggered within a predefined time frame. The ARSA developed at PNNL is one such detection system which has two separate beta and gamma detection channels. The ARSA system has demonstrated detection of ultra-low concentrations of the fission product radioxenon isotopes in several field tests (McIntyre et al., 2001 and 2006). With four gas cells, the ARSA system employs 12 PMTs for detecting coincident beta and gamma rays. This number of PMT's in one compact system requires a continuous and very accurate calibration.

We have studied phoswich detectors as a simple alternative system for measuring xenon radioisotopes. A phoswich detector consists of two or more scintillation layers which are optically coupled to a single photomultiplier tube. Generally, the plastic scintillation layer, close to the front window, detects less penetrating radiations such as beta particles, whereas the last layer close to the PMT is intended to measure more penetrating radiations such as high-energy gamma rays. Then the energy deposition in each layer, either in coincidence or singles, can be measured by using digital-pulse-shape discrimination techniques.

Considering the radioxenon detection requirements and current available manufacturing capabilities, a prototypic planar triple-layer phoswich detector was designed, modeled, and constructed (Farsoni and Hamby, 2006). The phoswich detector consists of a plastic scintillator (1.5 mm) for detection of beta and conversion electrons, a CaF_2 crystal (2.0 mm) for X-ray detection and a NaI(Tl) crystal (25.4 mm) for measuring gamma rays. The xenon gas cell in the final system is a thin hollow disk, 2-mm thick and 76.2 mm diameter, surrounded by two identical triple-layer phoswich detectors. The gas cell is completed by an aluminum sleeve which also joins the two detectors. To digitally capture the PMT's anode pulses from the two phoswich detectors, a two-channel digital pulse processor was designed and constructed. We also developed a GUI for controlling our digital processor, detecting coincidence events, and reconstructing beta/gamma spectra from the phoswich detectors. This paper will cover our digital pulse shape discrimination technique, the two-channel digital pulse processor (DPP2.0), the GUI, and our preliminary experiments with the prototypic phoswich detector.

RSSEARCH ACCOMPLISHED

Digital Pulse Shape Analysis

Depending on how the incident radiation releases its energy within each layer of the phoswich detector, seven possible pulse shapes or types could be generated at the PMT's anode output (Farsoni and Hamby, 2006). Using the following equations, and by employing three digital trapezoidal filters (Figure 1), we are able to discriminate different pulse shapes or interaction scenarios as depicted in Figure 2:

Fast Component Ratio (FCR) = Fa / Fb Equation 1

Slow Component Ratio (SCR) = (Fb-Fa) / (Fc-Fa) Equation 2

Where

Fa = Max(Pulse∗F1) Fb = Max(Pulse∗F2) Fc = Max(Pulse∗F3)

Pulse: Detector Response,
F1: Triangular Filter (40 ns peaking time),
F2: Triangular Filter (300 ns peaking time),
F3: Triangular Filter (4000 ns peaking time).

In the equations above, " ∗ " is a digital convolution operator and Max() indicates the amplitude of filter response. A triangular filter is a special trapezoidal filter with Gap=0. By using three digital triangular filters, F1, F2, and F3, with appropriate peaking times, we can integrate different areas of an anode pulse. These filters also automatically perform baseline corrections. Fa, Fb, and Fc indicate the amplitudes of corresponding filter response or integration values of each area in a given pulse. In another words, Fa, Fb and Fc represent integration of each pulse 40 ns, 300 ns and 4000 ns after the trigger point, respectively. The fast scintillation component from BC-400 (with ~40-50 ns duration by our fast digital pulse processor) will appear primarily in the first area, represented by Fa, whereas the slower scintillation component from NaI(Tl) (~ 230 ns decay constant) will appear mostly in the second area, represented by Fb. Fc will cover the slowest scintillation component from the CaF_2 (~ 900 ns decay constant).

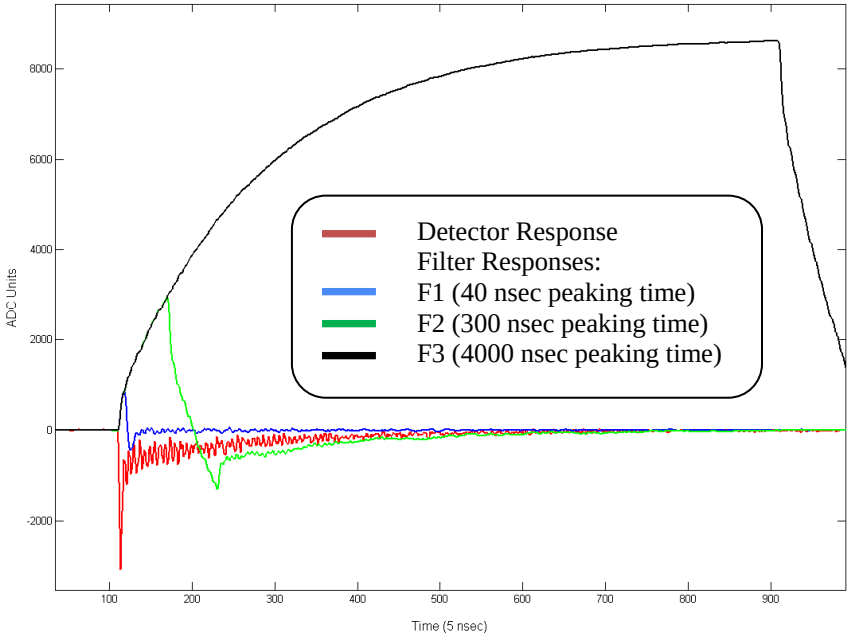

Figure 1. Digital trapezoidal filters are employed for pulse shape analysis of phoswich pulses. The anode trace in this graph was captured with a sampling rate of 200 MHz and cutoff frequency of 95 MHz in the digital processor (analog low-pass filter).

To discriminate between different pulse shapes, two ratios, FCR and SCR are calculated from each captured pulse. In Equations 1 and 2, the FCR and SCR range from zero to unity. Figure 2 shows a two-dimensional scatter plot of the FCR and SCR when the phoswich detector is exposed to a ^{137}Cs source. During this experiment, the ^{137}Cs source was shielded against beta and conversion electrons. Although the probability of occurrence of interaction scenarios are not same, by using this plot, the location of seven possible events or pulse shapes can be identified. Events from only BC-400 with high FCR are located in region1; these are mostly from Compton interactions from 662 keV of ^{137}Cs. The value of FCR for CaF_2-only and NaI-only events is low (0.1-0.2) and similar, but with different SCR. Therefore, these events are located in regions 2 and 4, respectively. Combined events from BC-400 and CaF_2 fall in region 3. Region 5 accommodates combined events from BC-400 and NaI. Region 6 indicates combined events from NaI and CaF_2. Events falling in region 7 are assumed to have more than two components. Table 1 summarizes the origin of each event and the corresponding scintillation layer for each region when the phoswich is used for radioxenon detection. In Table 1, pulses in regions 6 and 7 have no useful information for radioxenon detection and therefore are rejected. Rejection of events in region 6 will reduce the Compton background for low-energy gamma-ray detection since these events have been involved in a Compton scatter in the CaF_2 and then absorption or another Compton scatter in the NaI or vice versa.

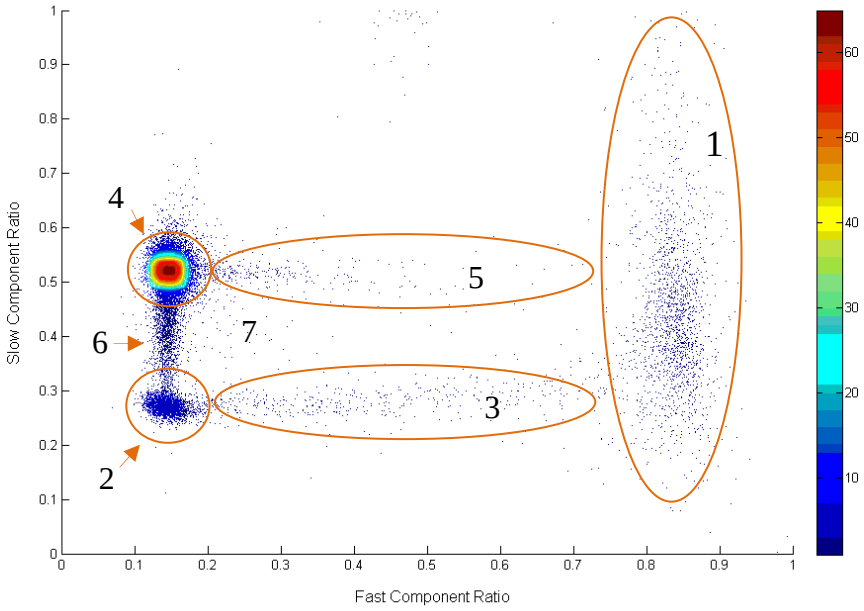

Figure 2. Scatter of FCRs and SCRs from ^{137}Cs. Seven marked regions correspond to seven pulse shapes, indicating how gamma rays interact with the three layers of phoswich detector. See Table 1 for more detail when this scatter plot is used for radioxenon detection.

Table 1. Seven pulse-type regions in Figure 2 and their corresponding layers and events when the phoswich detector is used for measuring xenon radioisotopes.

Region	Layer(s)	Event
1	BC-400	Beta/CE
2	CaF_2	X-Ray
3	CaF_2 + BC-400	Coincidence X-Ray, Beta/CE
4	NaI	Gamma-Ray
5	NaI + BC-400	Coincidence Gamma-Ray, Beta/CE
6	NaI + CaF_2	Rejected
7	NaI + CaF_2 + BC-400	Rejected

Figure 3 shows two FCR/SCR scatter plots, once when the phoswich detector is exposed to ^{99}Tc and again when exposed to ^{90}Sr/^{99}Y. The beta particles from ^{99}Tc always interact with the BC-400 (maximum energy of 293 keV). Therefore, region 1 is highly populated. In Figure 3b, some beta particles from ^{90}Sr/^{90}Y have enough energy to pass through the BC-400 layer and interact with the CaF_2 layer. Therefore, regions 1 and 3 are more populated. There is a small fraction of events in region 2 which could be due to pulses with very small fast components. In both scatter plots, there is also a small fraction of events in region 4; these are assumed to be due to background gamma rays interacting in the NaI layer.

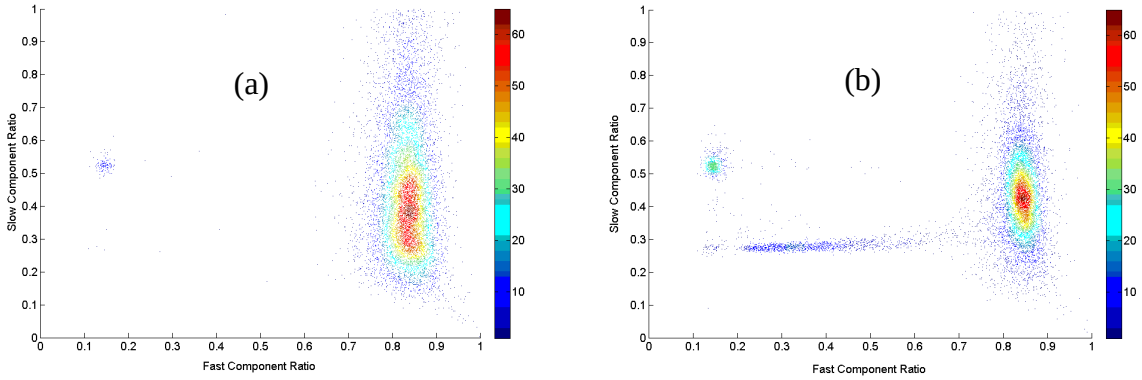

Figure 3. Distribution of FCRs and SCRs from (a) ^{99}Tc and (b) ^{90}Sr/^{90}Y.

Two-Channel Digital-Pulse Processor

A two-channel, high-speed (250 MHz) and compact (6.0 X 7.5 cm) DPP2.0 was designed and constructed for radoixenon analysis (Figure 4). The system benefits the new fast- and high-performance ADC's from analog devices (AD9230-250) with a sampling rate of 250 MHz and a resolution of 12 bits. The ADC consumes only 434 mW at its rated frequency. Such a very high sampling rate allows us to provide a more in-depth analysis of the signal pulses in which three timing components are possible. The ADC data bus uses the high performance Low-Voltage Differential Signaling (LVDS) standard. The offset and gain of each channel are controlled separately and digitally by our GUI software. The adjustable amplification gain for each channel ranges from -14 to +46 dB. A 3rd order, low-pass Bessel filter is used on board to attenuate high-frequency components in the signal pulses; the cut-off frequency of this filter is 95 MHz.

All the digital modules and functions such as trigger logic, circular buffer, digital trapezoidal filters, pile-up rejection, and coincidence detection are implemented in a 1500K gate-equivalent SPARTAN-3 FPGA from the Xilinx Incorporated. The on-board FPGA is automatically programmed via a high-speed USB2.0 port when the processor is connected to the PC. Once the FPGA is programmed (in about 30 msec), the high-speed USB2.0 interface is used either for controlling the processor or transferring data. The board is equipped with a 20-pin header interface to support a small LCD display for our future projects, when the board can be employed without using the PC.

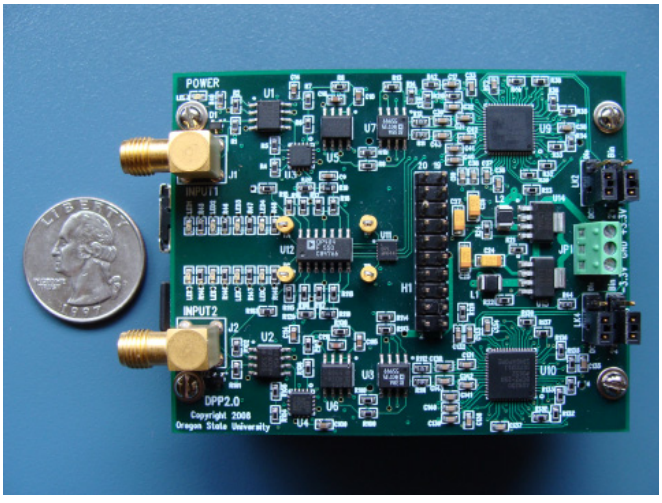

Figure 4. The top side of high-speed (250 MHz, 12-bit) and compact (6.0 X 7.5 cm) 2-channel DPP2.0 designed in our laboratory.

Graphical User Interface

A GUI was developed to control the DPP2.0 and radioxenon measurements (Figure 5). The GUI is written in Python programming language and was developed with the wxPython GUI toolkit. Through the software interface, the user can specify data-collection time (either live or real time), trigger threshold, gain, offset, coincidence window, pulse-shape discrimination parameters, and energy calibration coefficients. All of these parameters can be set separately for each channel. At this stage, the GUI is intended for prototyping purposes.

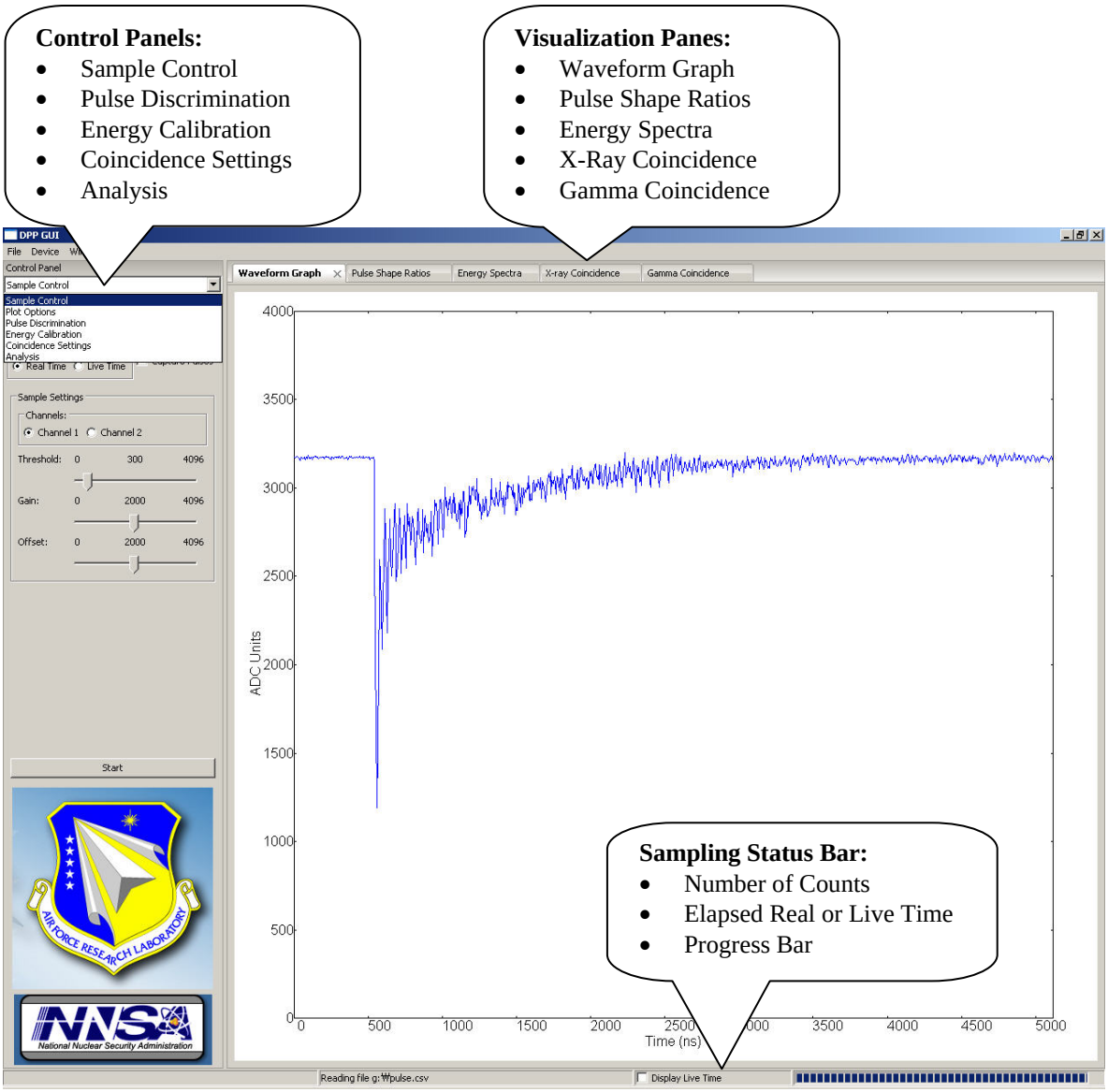

Figure 5. A snapshot from the GUI for controlling the DPP2.0, pulse shape analysis and reconstructing beta/gamma coincidence spectra. The GUI is under development in our laboratory at Oregon State University.

The user can direct the DPP2.0 to sample for a desired time (live or real) or number of counts through the software. During a sampling session, the GUI polls the FPGA for incoming data. When pulse data is received, the software

applies the three triangular filters to determine its FCR and SCR. Using the ratio information, the software tries to categorize the pulse into one of the five user-defined regions. Once the pulse type has been determined, the filter responses are used to calculate its energy content based on calibration coefficients for each of the different scintillator materials. Pulse type and energy are then used to produce energy histograms. The user may specify regions of interest on the histograms where the software calculates peak energy and full width half maximum (FWHM). To reduce memory usage on the host PC, the GUI discards the pulse waveforms, but saves the filter responses from each event. Hence, the effect of changing calibration and discrimination parameters can be observed without needing to begin a new sampling session. Filter widths and pre-processing parameters such as gain, offset, and threshold can also be set through the GUI, but those changes will only apply to future pulses. If further offline processing is desired, with MATLAB for example, the option to save pulse data to disk in comma separated values (CSV) format is available. The FPGA can also be reprogrammed from within the GUI if several variants of the FPGA code are to be tested. In the following, some key features of the GUI are given.

Visualization Panes

The GUI software has five visualization panes which are selectable via tabs along the top of the interface (see Figure 5).

Waveform Graph. This pane acts as an oscilloscope for displaying individual anode pulses from each phoswich detector. By using this pane and monitoring the anode pulses, the gain and offset for each channel can be adjusted to optimize sampling conditions.

Pulse Shape Ratios. This pane contains a scatter plot of FCR versus SCR for all pulses received in the sampling session.

Energy Spectra. This pane contains three energy histograms corresponding to the energy spectra of three scintillator layers. These spectra are updated from events in regions 1, 2 and 4 shown in Figure 2.

X-ray Coincidence. This pane has two portions (not shown). The top portion of this pane contains a 2-D scatter plot of beta versus X-ray energy for pulses categorized as BC-400/CaF_2 coincidence events. The bottom section is a spectrum of beta energies for a specific X-ray gating energy range. This pane is provided to monitor coincidence events in the 30 keV region of the coincidence spectra.

Gamma Coincidence. This pane is identical to the X-ray coincidence pane, but it displays information for pulses categorized as BC-400/NaI coincidence events.

Control Panel

The left sidebar (see Figure 5) is the GUI control panel with six pages (see Figure 6 a through f), selectable via a drop-down list:

Sampling Control (Figure 6a).In this panel, the user specifies the parameters for the sampling session. The session may be set to run for a specific real or live time, or until a certain number of pulses are acquired. For each channel of the DPP, threshold, gain, and offset can be set using sliders. The option is available to save captured pulse data to disk in CSVs format for offline processing.

Plot Options (Figure 6b). This page has options to toggle the display of each channel's output and to set channel colors, rescaling the axes for the waveform graph and the pulse-shape ratio plot, and setting the update interval, which specifies how often the ratio plot and histograms are redrawn. Plots can also be exported as graphics and saved to disk via this page.

Pulse Discrimination (Figure 6c). Here, the user can set the peaking time or the width of the fast-, medium-, and slow-pulse-shape discrimination filters. For a given peaking time of T_p, the resulting filter has $N = T_p.F_s$ taps with coefficients of -1 followed by N taps with coefficients of 1; F_s is the sampling rate of ADC. The five pulse discrimination regions are also set here. For each region, the mouse can be used to select a rectangular area of the pulse-shape ratio plot where that type of pulse is expected.

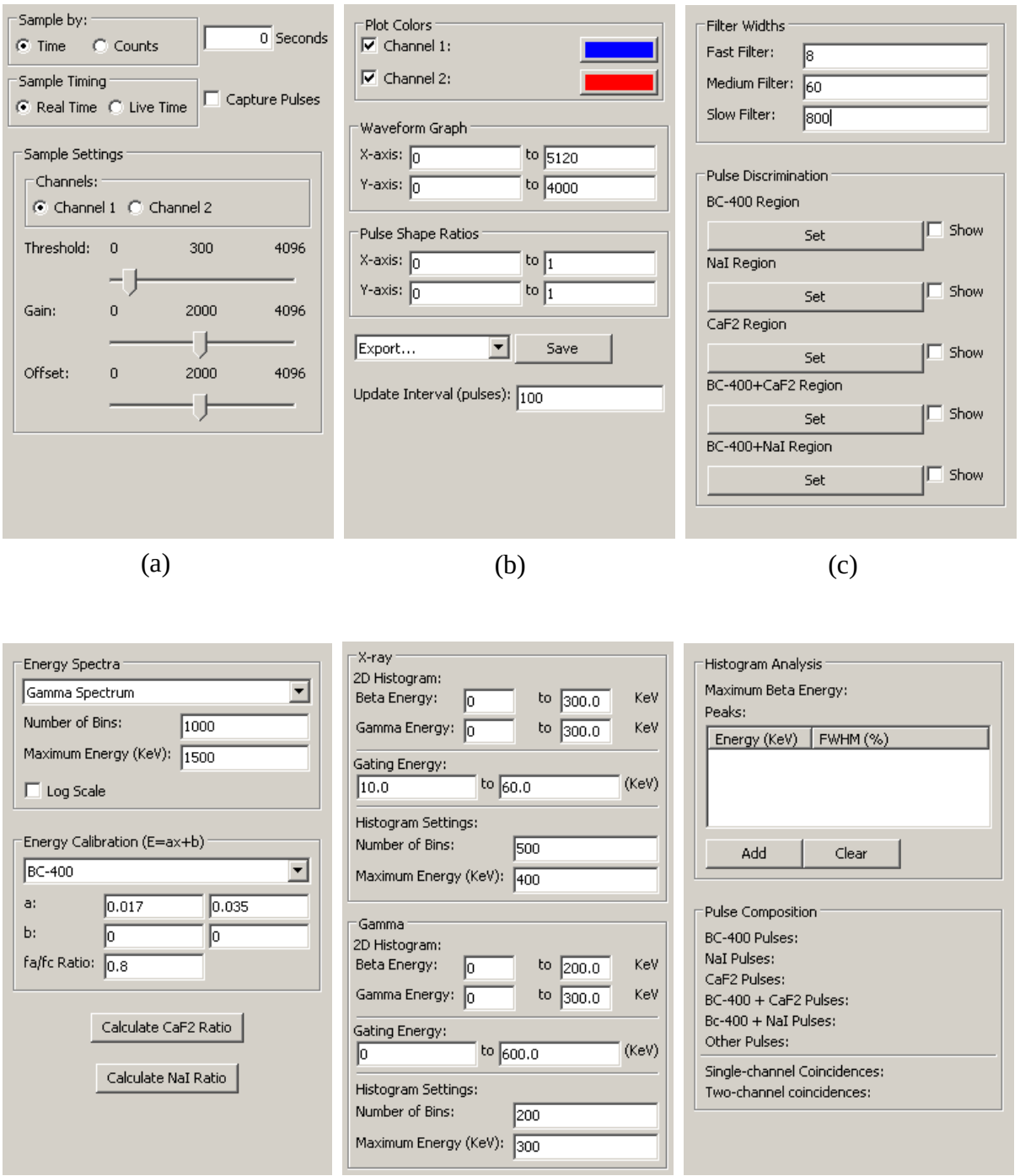

Figure 6. Six control panels selectable via a drop-down list from the main screen (see Figure 5).

Energy Calibration (Figure 6d). This page contains controls for the histogram settings in the energy-spectra display pane. For each spectrum, maximum energy and number of bins can be specified, and the counts axis can be toggled between linear and logarithmic. The energy calibration coefficients can be set here, individually for each channel and scintillation layer. There are also two buttons in this panel to calculate the CaF_2 and NaI correction factors.

These correction factors are used to extract the fast component from a combined pulse, that of either CaF_2/BC-400 or NaI/BC-400.

Coincidence Settings (Figure 6e). This page controls the two coincidence display panes. For each pane, the axes of the histograms can be rescaled and the number of bins in the energy spectrum can be set. The gating energy range for each coincidence spectrum can be set here.

Analysis (Figure 6f). At the end of the sampling session, the analysis page is populated with information about pulse composition, coincidence occurrences, and maximum beta energy recorded. Here, regions of interest can be selected in the energy spectra and the software will calculate peak energy and full width half maximum.

Other Features

During sampling, the bottom status bar shows the number of pulses recorded, the amount of time (real or live) elapsed, and a progress bar. Dialogs are available from the top menu for reprogramming the FPGA. Saved pulse data can be re-imported to be reprocessed with different parameters such as filter width.

Preliminary Measurements

Because of the hygroscopic nature of the NaI, this crystal must be isolated from other parts of the detector by an optical quartz layer. Our radiation transport modeling (Farsoni and Hamby, 2006) showed that the 30 keV X-ray is significantly attenuated by the quartz. Thus, to compensate this effect, a CaF_2 layer was added to the phoswich design to detect 30 kev X-rays from xenon radioisotopes. Regarding its slow decay constant and relatively low-light yield, detection and discrimination of 30-keV X-ray pulses produced from this layer was challenging.

A source of ^{133}Ba was used to find the optimum trigger parameters (e. g., duration of digital fast filter implemented in FPGA for triggering the system) in detecting and resolving X-ray and gamma rays. The ^{133}Ba source emits X-rays (31 keV) and gamma-rays (81, 303, and 356 keV) with energies close to those of the xenon radioisotopes of interest (31, 80 and 250 keV). By processing events in regions 2 and 4 of Figure 2, the energy spectra from CaF_2 and NaI were obtained. The two energy spectra are depicted in Figures 7a and 7b, respectively.

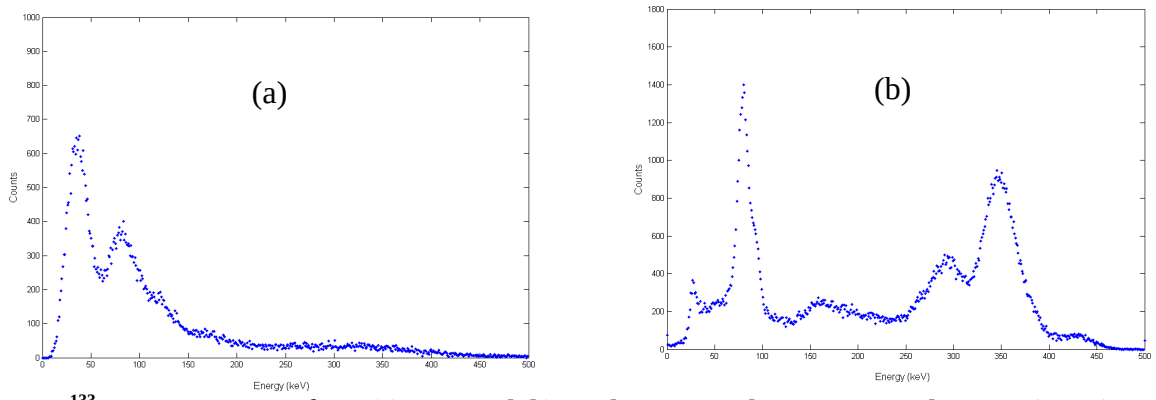

Figure 7. ^{133}Ba energy spectra from (a) CaF_2 and (b) NaI layers. For these spectra, only events in regions 2 and 4 of Table 1 were digitally processed, respectively.

In the CaF_2 spectrum (Figure 7a), the FWHM for 30 keV X-ray peak is 55% and is well separated from the 81 keV gamma-ray peak. The 30 keV peak can be also seen in the NaI spectrum in Figure 7b; with a significant attenuation which was predicted by our MCNP modeling (Farsoni et al., 2007). The 81 keV peak in the NaI spectrum has a FWHM of 17%. Other gamma-rays with higher energies from ^{133}Ba, such as 303 keV and 356 keV, are also prominent in this spectrum. There is also a peak from 276 keV gamma-ray which is overlapped with the 303 keV peak. At the time this paper was prepared, radioactive xenon gas was not available to test and characterize the phoswich detector for beta/gamma coincidence measurements.

CONCLUSION

We have developed a two-parameter digital-pulse-shape analysis technique to discriminate different pulse shapes from the three layers of our phoswich detector. We have also designed and constructed a fast and compact two-channel DPP2.0 to digitally process the anode pulses from our two-channel triple-layer phoswich detector. All the digital modules and functions are implemented in a 1500K gate-equivalent SPARTAN-3 FPGA from the Xilinx Incorporated. A GUI has been developed to control the digital processor and to digitally analyze phoswich pulses. Features to be added in the GUI include concentration calculations using regions of interest, background stripping considering the memory effect, and triple coincidence display. The preliminary experiments with ^{133}Ba showed that the use of CaF_2 in the phoswich design significantly increases the efficiency of the detector in measuring 30 keV X-rays from xenon radioisotopes. This experiment qualitatively demonstrated the digital pulse shape analysis technique and confirmed our previous MCNP modeling. Our future work includes use of commercially available radioxenon gas (^{133}Xe) to test and characterize the detection system for beta/gamma coincidence measurements. We are also currently working to produce a measurable amount of fission-product radioxenons by irradiating a highly enriched uranium foil in the Oregon State University's TRIGA reactor.

REFERENCES

McIntyre, J. I., K. H. Able, T. W. Bowyer, J. C. Hayes, T. R. Heimbigner, M. E. Panisko, P. L. Reeder, and R. C. Thompson (2001). Measurements of ambient radioxenon levels using the automated radioxenon sampler/analyzer (ARSA), *J. Radioanal. Nucl. Chem.* 248: 3, 629–635.

McIntyre, J. I., T. W. Bowyer, and P. L. Reeder (2006). Calculation of minimum detectable concentration levels of radioxenon isotopes using the PNLL ARSA system, Technical Report, PNNL-13102 (March 2006).

Farsoni, A. T. and D. M. Hamby (2006). Study of a triple-layer phoswich detector for beta and gamma spectroscopy with minimal crosstalk, in *Proceedings of the 28th Seismic Research Review: Ground-Based Nuclear Explosion Monitoring Technologies*, LA-UR-06-5471, Vol. 2, pp. 794–792.

Farsoni, A. T., D. M. Hamby, K. D. Ropon, and S. E. Jones (2007). A two-channel phoswich detector for dual and triple coincidence measurements of radioxenon isotopes, in *Proceedings of the 29th Monitoring Research Review: Ground-Based Nuclear Explosion Monitoring Technologies*, LA-UR-07-5613, Vol. 2, pp. 747–756.